Available online at www.sciencedirect.com

ScienceDirect

www.elsevier.com/locate/jes

JES JOURNAL OF ENVIRONMENTAL SCIENCES

www.jesc.ac.cn

Metabolomic profiles in a green alga (*Raphidocelis subcapitata*) following erythromycin treatment: ABC transporters and energy metabolism

Jiezhang Mo[1,2], *Zhihua Ma*[1], *Shiwei Yan*[1], *Napo KM Cheung*[2], *Fangshe Yang*[1], *Xiunan Yao*[1], *Jiahua Guo*[1,*]

[1] *Shaanxi Key Laboratory of Earth Surface System and Environmental Carrying Capacity, College of Urban and Environmental Sciences, Northwest University, Xi'an 710127, China*

[2] *State Key Laboratory of Marine Pollution and Department of Chemistry, City University of Hong Kong, Kowloon, Hong Kong, China*

ARTICLE INFO

Article history:
Received 29 July 2021
Revised 1 December 2021
Accepted 1 December 2021
Available online 23 February 2022

Keywords:
Hormesis
Metabolome
ABC transporters
DNA replication
Microalgae
Macrolide antibiotic

ABSTRACT

A recent study showed that erythromycin (ERY) exposure caused hormesis in a model alga (*Raphidocelis subcapitata*) where the growth was promoted at an environmentally realistic concentration (4 μg/L) but inhibited at two higher concentrations (80 and 120 μg/L), associated with opposite actions of certain signaling pathways (e.g., xenobiotic metabolism, DNA replication). However, these transcriptional alterations remain to be investigated and verified at the metabolomic level. This study uncovered metabolomic profiles and detailed toxic mechanisms of ERY in *R. subcapitata* using untargeted metabolomics. The metabolomic analysis showed that metabolomic pathways including ABC transporters, fatty acid biosynthesis and purine metabolism were associated with growth promotion in algae treated with 4 μg/L ERY. An overcompensation was possibly activated by the low level of ERY in algae where more resources were reallocated to efficiently restore the temporary impairments, ultimately leading to the outperformance of growth. By contrast, algal growth inhibition in the 80 and 120 μg/L ERY treatments was likely attributed to the dysfunction of metabolomic pathways related to ABC transporters, energy metabolism and metabolism of nucleosides. Apart from binding of ERY to the 50S subunit of ribosomes to inhibit protein translation as in bacteria, the data presented here indicate that inhibition of protein translation and growth performance of algae by ERY may also result from the suppression of amino acid biosynthesis and aminoacyl-tRNA biosynthesis. This study provides novel insights into the dose-dependent toxicity of ERY on *R. subcapitata*.

Introduction

The extensive use of antibiotics in medical treatments and aquaculture has led to a pressing environmental pollution issue (Martinez, 2009). Many classes of antibiotics, such as macrolides, lincosamides, sulfonamides, fluoroquinolones etc., have been frequently detected in different environmental compartments and biota on a global scale. Moreover, their adverse effects on both target and non-target organisms have been reported as well, raising environmental and public health concerns. (Guo et al., 2015, 2016; Kumar et al., 2019; Li et al., 2020; Zainab et al., 2020).

* Corresponding author.
E-mail: jiahua_guo@nwu.edu.cn (J. Guo).

https://doi.org/10.1016/j.jes.2021.12.001
1001-0742/

As a macrolide antibiotic, erythromycin (ERY) can act effectively against Gram-positive bacteria, and it is a commonly prescribed medicine for treating respiratory tract infection (Gaynor and Mankin, 2003; Shafia et al., 2016). After being prescribed and used by human and animals, ERY residues (ERY metabolites and approximate 5% of the parent compounds) are generally excreted into the sewage system and received by the wastewater treatment plants (WWTPs) (Miao et al., 2004). Due to the high resistance to treatment processes in WWTPs, ERY residues are ultimately discharged into the environment with effluents and sludges (Schafhauser et al., 2018). ERY has been reported to present in different environmental matrices around the world, and detected concentrations of ERY in surface water were up to 75.5 μg/L (Agunbiade and Moodley, 2014; Bai et al., 2014; Lin and Tsai, 2009; Valcárcel et al., 2011).

ERY can effectively inhibit the growth of bacteria (target organisms) through suppressing protein synthesis (Arenz et al., 2014; Jelić and Antolović, 2016); however, due to the development of antibiotic resistance in bacteria and high toxicity on non-target aquatic organisms caused by ERY, it has been identified as a high-risk substance for prioritization by the European Union since 2015 (Guo et al., 2015; Loos et al., 2018). Notably, algae, the primary producers, are more sensitive to ERY than crustaceans, bivalves, fish, and other non-target organisms in the food chains (Aguirre-Martińez, et al., 2016; Deng et al., 2014; Liang et al., 2020; Liu et al., 2011a, 2011b, 2014; Nie et al., 2013; Rodrigues et al., 2016, 2019; Sendra et al., 2018; Wan et al., 2015). For instance, ERY exposure for 72 hr inhibited growth of *Raphidocelis subcapitata* (*R. subcapitata*) at 38 and 200 μg/L, which was associated with altered cell biovolume and chlorophyll *a* content, as well as increased metabolic activity, augmented mitochondrial membrane potential and inhibited photosynthesis (Machado and Soares, 2019).

Notably, our recent studies showed that exposure of *R. subcapitat* to ERY caused hormesis in *R. subcapitata*. Specifically, the growth of *R. subcapitata* was promoted following 4 μg/L ERY treatment for 7 days, associated with activation of gene expression enriched in xenobiotic metabolism signaling and DNA replication signaling (Guo et al., 2021). On the contrary, algal growth inhibition observed at both 80 and 120 μg/L ERY treatments was correlated with suppression of signal pathways including xenobiotic metabolism, porphyrin and chlorophyll metabolism, and DNA replication (Guo et al., 2021); however, alterations at the metabolomic level in ERY-induced hormesis of *R. subcapitata* remain unclear.

Hormesis, a biphasic dose-response phenomenon indicated by stimulatory and inhibitory effects at low and high exposure doses of a stressor, respectively, is emerging as an important concept because it may challenge the current application of environmental risk assessment on chemicals (Calabrese, 2010). Indeed, a biphasic dose-response in hormesis is distinct from the linear non-threshold and threshold models that are commonly adopted in environmental risk assessment (Agathokleous et al., 2020). In-depth mechanistic studies on hormesis induced by environmental stressors (e.g., here ERY-induced hormesis in *R. subcapitata*) will enhance our understanding and generate constructive information for environmental risk assessment.

Metabolites are a set of cellular products generated by various biochemical reactions and controlled by protein activity and gene expression in an organism (Jamers et al., 2009; Li et al., 2019). Metabolomics, as a powerful bioanalytical tool in systems biology research, can generate important metabolic information for deciphering the altered regulatory metabolic networks by various stimuli (Aliferis and Jabaji, 2011; Jamers et al., 2009; Nägele, 2014). Therefore, metabolomics has been increasingly applied in assessing the toxicity of environmental pollutants, such as heavy metals, nanomaterials, antibiotics, etc., in aquatic organisms (Li et al., 2019; Matich et al., 2019; Peng et al., 2021; Slaveykova et al., 2021).

The present study aimed to assess the metabolomic profiles in *R. subcapitata* to identify potential cellular targets in algae to better understand the underlying processes in ERY-induced hormesis at an environmentally relevant concentration and algal growth inhibition in two higher ERY treatments. We hypothesized that there would be a dose-dependent dysregulation of metabolites involved in pathways including xenobiotic metabolism, porphyrin and chlorophyll metabolism, lipid metabolism, DNA replication, and energy metabolism in *R. subcapitata* following different ERY treatments. As a well-established dataset on the effects of antibiotics including ERY at half maximal effective concentration (EC_{50}) level is available for this species (Guo et al., 2015), the molecular mechanism of ERY revealed in this study has the potential to extrapolate to other antibiotics with similar mode of action.

1. Materials and methods

1.1. Chemicals and reagents

ERY (CAS# 114-07-8, HPLC ≥ 98%) was purchased from Tokyo Chemical Industry (Shanghai, China). Acetonitrile (CAS# 75-05-8) and methanol (CAS# 67-56-1) were purchased from Merck (Darmstadt, Germany). Ammonium acetate (CAS# 631-61-8) was purchased from Sigma-Aldrich (Missouri, USA). Ultrapure water (18.2 MΩ) was prepared using a Milli-Q purification system (Millipore, USA). All the chemicals used for the preparation of algal culture medium are at least reagent grade. A stock solution of ERY (10 mg/L) was prepared by dissolving ERY in Blue-Green (BG11) medium (Yoshinobu et al., 1983; Nie et al., 2013), followed by ultrasonication and membrane filtration (0.2 μm).

1.2. Algal cultivation and ERY treatments

A green microalga *R. subcapitata* (No. FACHB-271) was purchased from the Institute of Hydrobiology, Chinese Academy of Sciences (CAS, Wuhan, China). *R. subcapitata* is a recommended model algal species for ecotoxicological testing by the Organization for Economic Cooperation and Development (OECD) because it is widely distributed, ecologically important, fast-growing, easily cultivated, highly sensitive and whole genome sequenced (OECD, 2011; Suzuki et al., 2018). Cultivation of *R. subcapitata* and ERY treatments were performed as described previously (Guo et al., 2021). Briefly, algae (1.5×10^4 cells/mL) were seeded and cultured in 250 mL Erlenmeyer flasks filled with 150 mL Blue-Green (BG11) medium (pH

7.1). The inoculated algae were grown in a culture chamber under a 24 hr illumination of cool-white lights (~ 5500 lux light intensity) at (22 ± 2)°C. To facilitate CO_2 transfer and disperse the algae in culture medium, the cultures were shaken manually at least three times per day. To plot the growth curves, cell densities were determined using a multifunctional microplate reader at 680 nm and confirmed by cell counting using a haemocytometer.

R. subcapitata (1.5×10^4 cells/L) in the logarithmic growth phase were seeded in flasks containing 150 mL BG11 medium and exposed to ERY at a concentration of 4 (low; environmentally relevant concentration), 80 (medium; EC_{50}), and 120 μg/L (high; EC_{70}), respectively, for 7 days (Guo et al., 2021). Notably, our recently published data showed that ERY at concentrations up to 20 μg/L were able to induce hormesis in *R. subcapitata* (Ma et al., 2021). Algal cell densities were determined using a multifunctional microplate reader at day 2, 4, and 7. At the end of the ERY treatments, algae were harvested by centrifugation (9246 × *g*, 4°C, 10 min), snap frozen with liquid nitrogen, and kept at -80°C before the metabolomic analysis.

1.3. *Metabolomic analysis*

The metabolomic analysis was performed as described previously (Peng et al., 2021). Briefly, to extract metabolites from algae, a volume of 400 μL precooled mixed solution (methanol: acetonitrile: water = 4:4:2, V/V) were added to each sample, thoroughly mixed through vortex, and kept at -20°C for 60 min. After centrifugation (14,000 × *g*, 4°C, 20 min), the supernatants were collected and dried in vacuum. A volume of 100 μL acetonitrile water solution (acetonitrile: water = 1:1, V/V)) was added to redissolve the dried extracts, followed by vortex and centrifugation (14,000 × *g*, 4°C, 15 min).

Each sample was then separated using an ultra-high performance liquid chromatography (UHPLC) HILIC column (1.7 μm, 2.1 mm × 100 mm; Agilent Technologies, USA). The gradient program of UHPLC separation was shown in Appendix A **Table S1**. The separated samples were finally analyzed using a TripleTOF 6600 system (AB SCIEX, USA) coupled with electrospray ionization (ESI) source under positive mode and negative mode. Equal aliquots of each sample (10 μL) were pooled and mixed as the quality control (QC) sample to monitor the stability of the machine and reliability of data generated. Samples (including the QC sample) were randomly analyzed at 4°C.

The original data was converted into mzXML format by ProteoWizard, and the XCMS program was used for peak alignment, retention time correction and peak area extraction. Afterwards, identification of metabolites was achieved through referring to the primary information of mass spectra and matching of the secondary information in the online database METLIN. Multidimensional statistical analysis including unsupervised principal component analysis (PCA) and supervised orthogonal partial least squares discriminant analysis (OPLS-DA) were performed using the software SIMCA-P 14.1 (Umetrics, Umea, Sweden). In addition, a permutation test was performed 200 times to assess the risk of over-fitting for the applied model (Appendix A **Fig. S1**). Features with a variable importance on projection (VIP) value greater than 1 were then analyzed using Student's *t*-test, and metabolites with a p value < 0.05 were considered as differentially accumulated metabolites (DAMs). Volcano plots were depicted using R. Finally, all the DAMs identified through both positive and negative ion modes were combined for KEGG pathway analysis using MetaboAnalyst (Peng et al., 2021).

1.4. *Integrated analyses of transcriptomics and metabolomics data*

Both DAMs and their related genes were extracted from the KEGG compound and KEGG orthology database (https://www.kegg.jp/dbget-bin/www_bfind?compound). The expression levels of DAMs were then compared with their related genes with a $p < 0.05$ in the transcriptomics data published recently (Guo et al., 2021). Finally, the regulatory metabolomic pathways were generated by mapping DAMs and their related genes to the KEGG pathway database (Kanehisa et al., 2016).

1.5. *Statistical analysis*

Data statistical analysis was performed using GraphPad Prism 9.0. Statistical differences between ERY treatments and control were compared using a one-way analysis of variance (ANOVA) followed by Dunnett's post hoc test. A p value < 0.05 was considered statistically significant and indicated using an asterisk (*).

2. Results

2.1. *Growth performances of* R. subcapitata *following ERY treatments*

Growth performances of *R. subcapitata* following different ERY treatments (**Fig. 1**) were consistent with our previous study (Guo et al., 2021). Growth promotion in algae was observed in the 4 μg/L ERY treatment compared to the control, whereas algal growth in the 80 and 120 μg/L ERY treatment groups were both inhibited. Specifically, at day 7 the average algal cell density of the 4 μg/L ERY treatment was 15.9% greater than that in the control. By contrast, algal cell density was significantly ($p < 0.05$) reduced by 65.4% and 73.2% in the 80 and 120 μg/L ERY treatment, respectively.

2.2. *Metabolomic profiles altered by ERY treatments*

In total, 372 and 1395 metabolites were identified in the positive mode and negative mode, respectively (data not shown). In order to characterize the variation of metabolic profiles in samples of control and ERY treatments, unsupervised PCA was performed (Appendix A **Fig. S2**). PC1 and PC2 explains 46.3% (45.3%) and 11.5% (11.1%) of the total variance in metabolites detected by positive mode (negative mode), respectively. The good repeatability of QC sample data indicates that the metabolomic analysis in the present study was of high quality. In PCA score plots, replicates of the same treatment were clustered. Additionally, metabolomic profiles in the control were closed to the 4 μg/L ERY treatment group but were separated from the 80 and 120 μg/L ERY treatments. This observation is in agreement with growth performances of *R. subcapitata* in response to different ERY treatments where algal

Table 1 – Key metabolomic pathways ($p < 0.05$) in *R. subcapitata* altered by exposure to 4 μg/L erythromycin.

Pathway name	Pathway ID	*p* Value	Up-DAMs	Down-DAMs
Purine metabolism	cre00230	0.0023	Adenine, Urate	Deoxyadenosine, Xanthosine
Fatty acid biosynthesis	cre00061	0.0048	Decanoic acid, Octadecenoic acid, Octadecanoic acid	–
ABC transporters	cre02010	0.0083	Adenine, Urate, Taurine	Deoxyuridine, Deoxyadenosine, Xanthosine

DAMs: differentially accumulated metabolites. A dash (–) indicates no up- or down-DAMs in a specific metabolomic pathway.

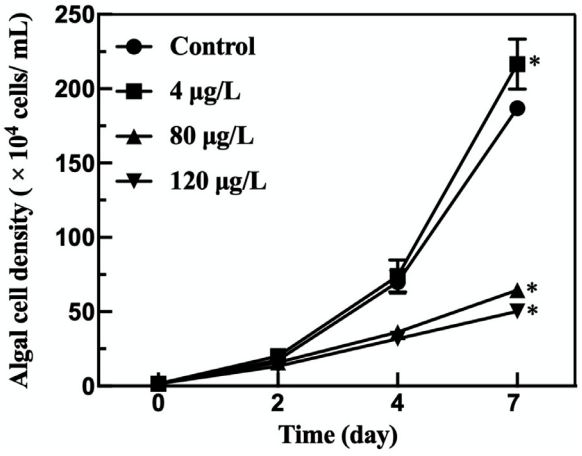

Fig. 1 – Growth performances of *R. subcapitata* in the inhibition test following different erythromycin (ERY) treatments for 7 days. Data are presented as mean ± standard deviation ($n = 3$). An asterisk (*) indicates significant difference ($p < 0.05$) between the ERY treatment and the control, analyzed by one-way ANOVA following Tukey's post hoc test.

growth was promoted at 4 μg/L but inhibited at 80 and 120 μg/L (Fig. 1).

In the supervised OPLS-DA, the R2Y values and Q2 values were 0.999–1 (> 0.5) and 0.984–0.999 (> 0.5), respectively, suggesting a high reliability of the model applied. Additionally, a distinct separation was observed in metabolomics profiles under both modes between the control and ERY treatment groups (Appendix A **Fig. S3**). Using VIP > 1 and $p < 0.05$ (according to Student's *t*-test) as threshold, a total of 72 (37 up-regulated, 35 down-regulated), 178 (94 up-regulated, 84 down-regulated), and 200 (106 up-regulated, 94 down-regulated) DAMs were identified in the positive mode, in the 4, 80 and 120 μg/L ERY treatment, respectively. In the negative mode, there were 232 (110 up-regulated, 122 down-regulated), 772 (196 up-regulated, 576 down-regulated), and 823 (199 up-regulated, 624 down-regulated) DAMs identified in algae treated with 4, 80 and 120 μg/L ERY, respectively (Appendix A **Fig. S4**).

All the DAMs detected in positive and negative ion mode in each ERY treatment were combined and submitted to the KEGG website for pathway analysis. A total of 6, 20, and 19 KEGG pathways were significantly ($p < 0.05$) altered in the 4, 80 and 120 μg/L ERY treatments, respectively (Tables 1-3 and Appendix A **Table S2**).

2.3. *Integrated analyses of ERY-altered metabolome and transcriptome*

The integrated analyses of transcripts and metabolites showed that a total of 8, 44, and 55 DAMs were found to be paired with a least one transcript in the 4, 80 and 120 μg/L ERY treatment group compared to the control, respectively (Appendix A **Tables S3-S5**). Most of these DAMs were enriched in multiple KEGG metabolic pathways, such as ABC transporters, 2-oxocarboxylic acid metabolism, glyoxylate and dicarboxylate metabolism, biosynthesis of amino acids, aminoacyl-tRNA biosynthesis, pyrimidine metabolism, purine metabolism, fatty acid biosynthesis, etc.

3. Discussion

This study elucidated the toxic mechanism(s) of ERY to *R. subcapitata* at the metabolic level. In accordance with our hypothesis, a dose-dependent dysregulation of metabolic pathways including ABC transporters, metabolism of carbohydrates and amino acids, lipid metabolism, and metabolism of purines and pyridines was evident in *R. subcapitata* following different ERY treatments. These findings enable a better understanding on the mechanisms of hormetic effect in algae treated with ERY at an environment-related level (4 μg/L ERY) and algal growth inhibition in the 80 and 120 μg/L ERY treatments. Although the ERY exposure concentrations were not determined during the exposure in the present study, a previous study reported that there were 95% (± 3.5%) and 87% (± 4.7%) of the initial ERY (60–300 μg/L) in the exposure medium at 24 and 96 hr, respectively, after *R. subcapitata* was treated with ERY, which suggests that ERY was relatively stable during the exposure experiments (Nie et al., 2013). Under the prolonged exposure of ERY (along with its degraded products possibly generated through hydrolysis, photolysis or biodegradation), hormesis observed in *R. subcapitata* following different ERY treatments were likely attributed to the alterations in ABC transporters and energy metabolism.

3.1. *ATP-binding cassette (ABC) transporters*

ABC transporters are a transport system superfamily presenting in diverse species ranging from microorganisms to humans (Thomas et al., 2020). ABC transporters, as exporters

Table 2 – Key metabolomic pathways ($p < 0.05$) in *R. subcapitata* altered by exposure to 80 μg/L erythromycin.

Pathway name	Pathway ID	*p* Value	Up-DAMs	Down-DAMs
ABC transporters	cre02010	0.0001	L-Arginine, Phosphate	Deoxyinosine, Deoxyadenosine, D-Glucose, Glycerol, L-Glutamate, L-Leucine, Sucrose, Taurine, Uridine, Xanthosine, Alanine, Proline, Isoleucine, Tryptophan, Glutamine
Biosynthesis of amino acids	cre01230	0.0001	D-Ribose 5-phosphate, L-Arginine	alpha-Isopropylmalate, 2-Oxoadipate, 3-Methyl-2-oxobutanoic acid, L-Glutamate, L-Leucine, Shikimate, Pyruvate, Alanine, Proline, Isoleucine, Tryptophan, Glutamine
Purine metabolism	cre00230	0.0003	Adenine, D-Ribose 5-phosphate, Urate, dGMP	dAMP, Deoxyadenosine, Xanthosine, Guanosine, Hypoxanthine, Inosine
2-Oxocarboxylic acid metabolism	cre01210	0.0005	Citrate, Isocitrate	alpha-Isopropylmalate, 2-Oxoadipate, 7-Methylthioheptyl glucosinolate, 8-Methylthiooctyl glucosinolate, 3-Methyl-2-oxobutanoic acid, L-Leucine, Isoleucine, Pyruvate, Tryptophan
Pyrimidine metabolism	cre00240	0.0021	3-Hydroxypropanoate, CDP, CMP, dCDP, Orotate	Uridine, Deoxyuridine, Pseudouridine, Uracil
Pantothenate and CoA biosynthesis	cre00770	0.0070	–	3-Methyl-2-oxobutanoic acid, Pantothenate, Pyruvate, Uracil
Fatty acid biosynthesis	cre00061	0.0089	Decanoic acid, Dodecanoic acid	Octadecenoic acid, Hexadecenoic acid
Glyoxylate and dicarboxylate metabolism	cre00630	0.0112	Citrate, Glycolate, Isocitrate	4-Hydroxy-2-oxoglutarate, L-Glutamate, Pyruvate, Succinate
Aminoacyl-tRNA biosynthesis	cre00970	0.0369	L-Arginine	L-Glutamate, L-Leucine, Alanine, Proline, Isoleucine, Tryptophan, Glutamine

DAMs: differentially accumulated metabolites. A dash (–) indicates no up- or down-DAMs in a specific metabolomic pathway.

or importers, are highly involved in the uptake of nutrients into cells and efflux of endogenous toxins and xenobiotics out of cells driven by the bioenergy released from ATP hydrolysis (Andolfo et al., 2015). Specifically, they transport various substrates across membranes extracellularly and intracellularly, such as amino acids, nucleotides, carbohydrates, lipid-related compounds (e.g., cholesterol, steroids), vitamins, peptides, glutathione conjugates, heavy metal chelates, and xenobiotics (e.g., antibiotics, herbicides) (Dahuja et al., 2021). In the present study, the metabolic pathway of ABC transporters was altered in all ERY treatments (**Tables 1-3**). In algae treated with 4 μg/L ERY, metabolites including amino acids (e.g., taurine) and nucleoside-related compounds (e.g., deoxyuridine, deoxyadenosine, xanthosine) were enriched in the metabolic pathway of ABC transporters (**Table 1**), while more metabolites such as carbohydrates (e.g., D-glucose, glycerol, sucrose), amino acid (e.g., taurine, L-arginine, L-glutamate, L-leucine, alanine, proline, isoleucine, tryptophan, glutamine) and nucleoside-related compounds (e.g., uridine, deoxyadenosine, xanthosine) were enriched in the 80 and 120 μg/L ERY treatments (**Tables 2-3**).

In plants such as algae, ABC transporters are localized in the membranes of different organelles (e.g., vacuoles, chloroplasts, mitochondria, peroxisomes), regulating diverse biological processes, such as cell growth, tolerance to environmental stresses and transport of secondary metabolites (Andolfo et al., 2015; Kang et al., 2011). Notably, downregulation of ABC transporter family genes was observed in the 80 μg/L (encoding ABCA, ABCG) and 120 μg/L (encoding ABCA, ABCB, ABCG, ABCI) ERY treatments (Guo et al., 2021). ABC transporter family A, B and G are involved in cellular lipid transport, auxin transport, resistance to stresses (e.g., pathogens, antibiotics, herbicides), respectively, but the functions of ABC transporter family I remain unknown (Andolfo et al., 2015; Kang et al., 2011). The consistent downregulation of ABC transporter family G gene in algae treated with 80 and 120 μg/L ERY may reduce the transport of substrates and endogenous toxins and xenobiotics.

3.2. *Metabolism of carbohydrates and amino acids*

Carbohydrates ($C_nH_{2n}O_n$, $n \geq 3$) and proteins, the most abundant organic molecules on the earth, form the structural and functional bases for all the living creatures, along with another two classes of organic compounds, lipids and nucleic acids (Ward and Thompson, 2012). Carbohydrates (e.g., glucose) serve as direct "cell fuels" and are oxidized to produce bioenergy stored in ATP (Hall and Mertens, 2017). They are also cellular energy-storing compounds (e.g., glycogen, starch) and structural component (e.g., chitin, cellulose) of cells (Dashty, 2013). By contrast, amino acids serve as building blocks of proteins and important metabolic intermediates (e.g., biosynthesis of porphyrins using glycine) (Akram et al., 2011). Notably, metabolism of carbohydrates and amino acids

Table 3 – Key metabolomic pathways ($p < 0.05$) in *R. subcapitata* altered by exposure to 120 μg/L erythromycin.

Pathway name	Pathway ID	*p* Value	up-DAMs	Down-DAMs
Pyrimidine metabolism	cre00240	0.0001	CDP, dCDP, 3-Hydroxypropanoate, Orotate	Cytosine, Deoxyuridine, Uridine, Pseudouridine, Uracil
2-Oxocarboxylic acid metabolism	cre01210	0.0003	Citrate, Isocitrate	alpha-Isopropylmalate, 2-Oxoadipate, 7-Methylthioheptyl glucosinolate, 8-Methylthiooctyl glucosinolate, 3-Methyl-2-oxobutanoic acid, L-Leucine, Isoleucine, Pyruvate, Tryptophan
ABC transporters	cre02010	0.0003	L-Arginine, Phosphate	Deoxyinosine, Deoxyuridine, L-Glutamate, L-Leucine, Uridine, Xanthosine, D-Glucose, Glycerol, Sucrose, Taurine, Alanine, Proline, Isoleucine, Tryptophan, Glutamine
Biosynthesis of amino acids	cre01230	0.0001	L-Arginine	alpha-Isopropylmalate, 2-Oxoadipate, 3-Methyl-2-oxobutanoic acid, L-Glutamate, L-Leucine, Shikimate, Pyruvate, Alanine, Proline, Isoleucine, Tryptophan, Glutamine
Pantothenate and CoA biosynthesis	cre00770	0.0039	–	3-Methyl-2-oxobutanoic acid, Pantothenate, Uracil
Purine metabolism	cre00230	0.0045	dGMP, Adenine	dAMP, Deoxyinosine, Xanthosine, hypoxanthine, Inosine, Guanosine
Aminoacyl-tRNA biosynthesis	cre00970	0.0215	L-Arginine	L-Glutamate, L-Leucine, Alanine, Proline, Isoleucine, Tryptophan, Glutamine
Fatty acid biosynthesis	cre00061	0.0287	Decanoic acid, Dodecanoic acid, Octadecanoic acid	Octadecenoic acid, Hexadecenoic acid
Glyoxylate and dicarboxylate metabolism	cre00630	0.0321	Citrate, Glycolate, Isocitrate	L-Glutamate, Pyruvate, Succinate
Linoleic acid metabolism	cre00591	0.0408	3-Sulfino-L-alanine, 5′-Methylthioadenosine	Arachidonate, Linoleate

DAMs: differentially accumulated metabolites. A dash (–) indicates no up- or down-DAMs in a specific metabolomic pathway.

are involved in a variety of molecular signaling pathways and biological processes, such as folding and stabilization of proteins, growth and division of cells, etc. (Ward and Thompson, 2012). In this study, multiple pathways related to metabolism of carbohydrates and amino acids, such as 2-oxocarboxylic acid metabolism, glyoxylate and dicarboxylate metabolism, biosynthesis of amino acids, Aminoacyl-tRNA biosynthesis, etc., were altered consistently in both the 80 and 120 μg/L ERY treatments (Tables 2-3).

The signaling pathway of 2-oxocarboxylic acid metabolism describes multiple reactions of chain extension and modification on 2-oxocarboxylic acids (e.g., pyruvate, 2-oxobutanoate, oxaloacetate and 2-oxoglutarate) using carbons derived from acetyl-CoA (Stottmeister et al., 2005). By contrast, the metabolism of glyoxylate and dicarboxylate involves a series of enzymatic reactions on glyoxylates and dicarboxylates, the conjugate bases of glyoxylic acid and dicarboxylic acids, respectively (Etienne et al., 2013). These two signaling pathways form tight connections with metabolism of carbohydrates, biosynthesis of amino acids, biosynthesis of coenzymes, etc. (Ward and Thompson, 2012). In particular, metabolites related to carbohydrates (e.g., pyruvate, succinate, citrate, isocitrate, glycolate) and amino acids (e.g., L-leucine, isoleucine, tryptophan, L-glutamate) were dysregulated in both the 80 and 120 μg/L ERY treatments (Fig. 2 and Tables 2-3). Pyruvate kinase (encoded by *pk*) catalyzes the reaction of ATP and pyruvate to generate ADP and phosphoenolpyruvate (Ambasht and Kayastha, 2002), while decarboxylation and dehydration of pyruvate is catalyzed by pyruvate decarboxylase (encoded by *pdc*) and pyruvate dehydrogenase (encoded by *pdhb*), respectively (Patel and Korotchkina, 2003). The reduction in contents of pyruvate was associated with the downregulation of *pk*, *pdc* and *pdhb*. In addition, citrate synthase (encoded by *cs*) can convert acetyl-CoA and oxaloacetate to citrate and CoA (Wiegand and Remington, 1986), while aconitate hydratase (encoded by *aco*) catalyzes the interconversion between citrate and cis-aconitate (Igamberdiev and Eprintsev, 2016). Increased contents of citrate and isocitrate may be due to the upregulation of *cs* and *aco* in the 80 and 120 μg/L ERY treatments (Appendix A **Tables S4-S5**). The dysregulation of glyoxylate and dicarboxylate metabolism likely altered carbon metabolism and reduced energy production, ultimately contributing to the algal growth inhibition.

In biosynthesis of amino acids, metabolites including alpha-isopropylmalate, 2-oxoadipate, 3-methyl-2-oxobutanoic acid, L-glutamate, L-leucine, alanine, proline, isoleucine, tryptophan, and glutamine were depleted in both the 80 and 120 μg/L ERY treatments (Fig. 2 and Tables 2-3).

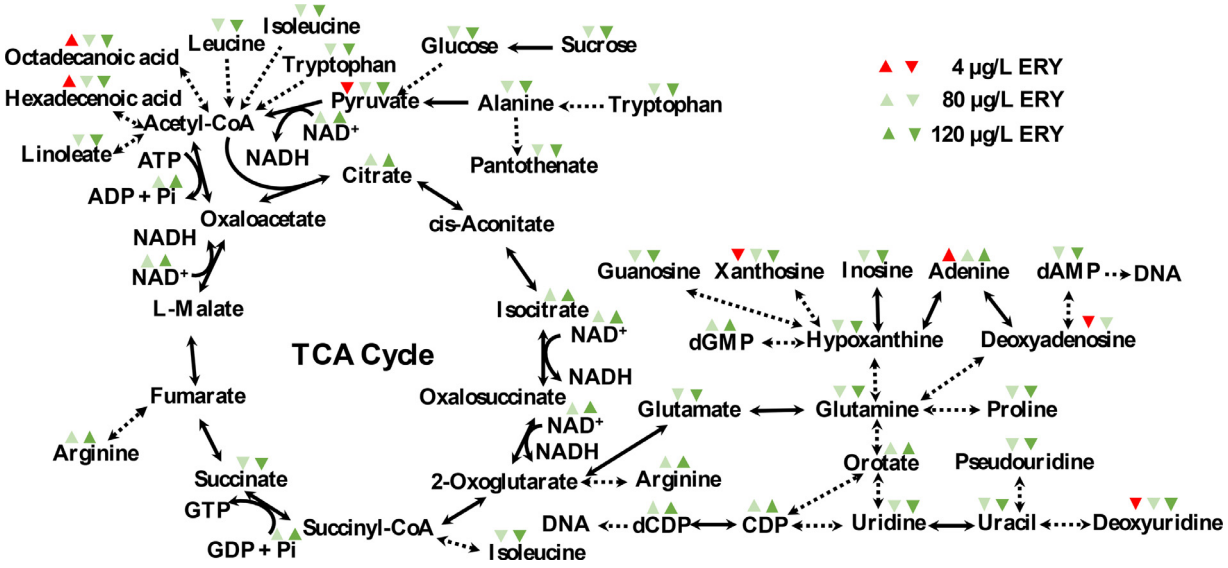

Fig. 2 – Metabolic networks altered by different erythromycin (ERY) treatments in *R. subcapitata*. An upright triangle and inverted triangle signifies the increased and reduced content of a specific metabolite, respectively. A solid arrow and dotted arrow indicates a direct and indirect reaction process between two metabolites, respectively.

Notably, aspartate aminotransferase catalyzes the reaction of L-aspartate and 2-oxoglutarate to generate oxaloacetate and L-glutamate (de la Torre et al., 2014). In addition, glutamate synthase (NADH) encoded by *glt1* can catalyze conversion of L-glutamate and NAD^+ to L-glutamine, 2-oxoglutarate and NADH (Lea and Miflin, 2003). In contrast, branched-chain amino acid aminotransferase (encoded by *E2.6.1.42*) catalyzes the reaction of L-leucine (or isoleucine) and 2-oxoglutarate to produce 4-methyl-2-oxopentanoate (or 3-methy-2-oxopentanoate) and L-glutamate (Binder et al., 2007). The downregulation of *got1* (encoding aspartate aminotransferase, cytoplasmic), *asp5* (encoding aspartate aminotransferase, chloroplastic), *glt1* and *E2.6.1.42* was possibly responsible for the depleted contents of L-glutamate, glutamine, L-leucin and isoleucine (Appendix A **Tables S4-S5**). The inhibition of amino acid biosynthesis again suggests that carbon metabolism and energy production might be impaired in algae with degraded growth performances.

Additionally, aminoacyl-tRNA is a product formed by an amino acid and its cognate tRNA, and aminoacyl-tRNA synthetases are responsible for the catalysis of these reactions during protein synthesis (Ibba and Söll, 2000). In aminoacyl-tRNA biosynthesis, there was consistent reduction in contents of amino acids (e.g., L-glutamate, L-leucine, alanine, proline, isoleucine, tryptophan, glutamine) in both the 80 and 120 μg/L ERY treatments (**Fig. 2** and **Tables 2-3**). In accordance with reduced contents of amino acids, downregulation of genes including *ears* (encoding glutamyl-tRNA synthetase), and *lars* (encoding leucyl-tRNA synthetase) was observed in the 80 μg/L ERY treatment (Appendix A **Table S4**), while *ears*, *lars* and *war* (encoding tryptophanyl-tRNA synthetase) were downregulated in the 120 μg/L ERY treatment (Appendix A **Table S5**). ERY is known to exert its toxicity through binding to the 50S subunit of ribosomes and inhibiting protein translation (Arenz et al., 2014; Jelić and Antolović, 2016). Novel data presented in this study suggest that ERY exposure suppressed the biosynthesis of amino acids and aminoacyl-tRNA biosynthesis, which may contribute to the suppression of protein translation and growth inhibition in both the 80 and 120 μg/L ERY treatments.

In accord with growth inhibition and the aforementioned reduction of metabolites related to carbohydrates and amino acids, NAD^+ and phosphate consistently increased in algae treated with 80 and 120 μg/L ERY (**Fig. 2** and **Tables 2-3**). NAD^+ serves as an essential redox co-factor in multiple energy metabolic pathways, such as respiration, photosynthesis, photorespiration, pentose-phosphate cycle, etc. (Xiao et al., 2018). In contrast, phosphate is essential constituents of bio-membranes (phospholipids), nucleic acids (DNA, RNA), bioenergy molecules (ATP, GTP), intracellular signaling molecules, etc. (Raghothama, 2000). Phosphate can be released from multiple metabolic processes including the hydrolysis of ATP (Kamerlin et al., 2013). Therefore, high levels of NAD^+ and phosphate accumulated in algal cells treated with high levels of ERY likely suggest a deficient in energy supply and alterations in redox status were likely occurred (Kamerlin et al., 2013; Xiao et al., 2018), leading to algal growth inhibition (Guo et al., 2021).

3.3. *Lipid metabolism*

Lipids are composed of sterols, waxes, mono/di-/tri-acylglycerols, fat-soluble vitamins, phospholipids, fatty acid. Lipids are building blocks of bio-membranes (e.g., phospholipids, glycolipids, cholesterol) and essential components of enzymes (vitamins A, D, E, K) (Guschina et l., 2006; Wan et al., 2020). Additionally, lipid metabolism is closely related to many biological processes including energy storage (tri-acylglycerols), reproduction (fat-soluble hormones), and cellular signaling (diacylglycerol, phosphatidylinositol-3,4,5-

trisphosphate) in plants including algae (Cagliari et al., 2011; Li-Beisson et al., 2019).

In this study, fatty acid biosynthesis was dysregulated in all ERY treatments (Tables 1-3). Metabolites including decanoic acid, octadecenoic acid, octadecanoic acid increased in the 4 μg/L ERY treatment (Fig. 2 and Table 1). By contrast, in both the 80 and 120 μg/L ERY treatments, decanoic acid and dodecanoic acid increased while octadecenoic acid and hexadecenoic acid decreased (Fig. 2 and Tables 2-3). Fatty acyl-ACP thioesterase A encoded by *fafa* hydrolyzes an acyl group of fatty acids and terminate the elongation during *de novo* fatty acid synthesis in plants (Voelker, 1996). In accordance with the promoted algal growth in the 4 μg/L ERY treatment, increased contents of octadecenoic acid were associated with the upregulation of *fafa* (Appendix A **Table S3**). By contrast, in algae treated with 120 μg/L ERY, growth inhibition of *R. subcapitata* was associated with a downregulation of *fafa* as well as a reduction in contents of octadecenoic acid and hexadecenoic acid (Appendix A **Table S5**). These novel findings suggest that opposite alterations in fatty acid biosynthesis were related to the dose-dependent ERY toxicity, promotion and inhibition of algal growth in the 4 μg/L and 120 μg/L ERY treatment, respectively.

In addition, the metabolic pathway of pantothenate and CoA biosynthesis was altered in both the 80 and 120 μg/L ERY treatments (Tables 2-3). In these two ERY treatments, contents of 3-methyl-2-oxobutanoic acid and pantothenate consistently decreased (Fig. 2 and Tables 2-3). Pantothenate kinase (encoded by *pank1_2_3*) converts ATP and pantothenate to ADP and D-4′-Phosphopantothenate (Raman and Rathinasabapathi, 2004). The reduction in contents of pantothenate in the 120 μg/L ERY treatment was associated with the downregulation of *pank1_2_3*, which suggests a suppression of pantothenate and CoA biosynthesis in the 120 μg/L ERY treatment (Appendix A **Table S5**). Notably, in algae treated with 120 μg/L ERY, contents of 3-sulfino-L-alanine, 5′-methylthioadenosine increased, while contents of arachidonate and linoleate decreased in the dysregulation of linoleic acid metabolism (Fig. 2 and Table 3). The dysregulation of lipid metabolism in the 80 and 120 μg/L ERY treatments might lead to excessive production of reactive oxygen species and ultimately contributed to the growth inhibition of *R. subcapitata* (Guo et al., 2021; Ma et al., 2021; Yalcinkaya et al., 2019).

3.4. *Metabolism of purines and pyridines*

Purines (i.e., adenine, guanine) and pyrimidines (i.e., cytosine, uracil, thymine) as essential components of nucleic acid (i.e., DNA, RNA), they preserve and transfer genetic information in all living creatures including algae (Chitrakar et al., 2017). In addition, purines and pyrimidines are also precursor molecules of energy storage depots (e.g., ATP, GTP), cell signaling regulators (e.g., cAMP, cGMP) and cofactors (e.g., NADH, NADPH, coenzyme A) of many enzymes (Stasolla et al., 2003). In this study, dysregulation of purine metabolism was observed in all ERY treatments (Tables 1-3), while metabolism of pyrimidine was only dysregulated in the 80 and 120 μg/L ERY treatments (Tables 2-3). Specifically, in purine metabolism, adenine, xanthosine and deoxyadenosine were consistently altered in all ERY treatments (Fig. 2 and Tables 1-3), while the contents of guanosine, inosine, hypoxanthine, dAMP and dGMP were modified in algae exposed to 80 and 120 μg/L ERY (Fig. 2 and Tables 2-3). In pyrimidine metabolism, metabolites including orotate, uridine, uracil, pseudouridine, CDP, dCDP and deoxyuridine were differentially accumulated in both the 80 and 120 μg/L ERY treatments (Fig. 2 and Tables 2-3). Alterations in metabolism of purine and pyrimidine suggest an intensive nucleotide metabolism in algae under ERY stress. This is consistent with the observations that signaling of DNA replication was activated in algae treated with 4 μg/L ERY, but inhibited DNA replication signaling in the 80 and 120 μg/L ERY treatments (Guo et al., 2021). Because metabolism of nucleotides can generate deoxyribonucleotides as building blocks for DNA replication and repair (Siddiqui and Ceppi, 2020), it is considered as a key pathway in ERY-caused hormesis in algae.

Adenine phosphoribosyltransferase (encoded by *aprt*) catalyzes the reaction between adenine and phosphoribosyl pyrophosphate (PRPP) to produce adenylate (AMP) and phosphate in the purine nucleotide salvage pathway (Moffatt et al., 1994). The downregulation of *aprt* is consistent with increased contents of adenine in all ERY treatments (Appendix A **Tables S3-S5**), which may serve as a negative feedback to the purine nucleotide salvage pathway. In addition, increased contents of adenine may be used to generate adenosine, an ingredient for synthesis of ADP and ATP. These findings suggest that purine metabolism was one of the initial targets of ERY toxicity, and the repair efficiency and strategies applied to these impairments probably lead to the dose-dependent effects of ERY on *R. subcapitata* (Calabrese, 2010). In addition, purine nucleosidase (encoded by *iunh*) and 5′-nucleotidase (encoded by *sure*) can convert nucleotides to the corresponding nucleosides (Burch and Stuchbury, 1987). The downregulation of *iunh* and *sure* was associated with the altered contents of adenine, xanthosine, inosine, guanosine, hypoxanthine, deoxyadenosine, dAMP and dGMP in the dysfunction of purine metabolism and growth inhibition in the 120 μg/L ERY treatment (Appendix A **Table S5**).

UMP-CMP kinase (encoded by *cmpk1*) plays a key role in the *de novo* biosynthesis of pyrimidine nucleotides where it catalyzes the reaction of pyrimidine nucleoside monophosphates and ATP to generate pyrimidine nucleoside diphosphates and ADP (Kafer et al., 2004). The downregulation of *cmpk1* may be related to elevated contents of nucleoside diphosphates in the 80 μg/L (CDP, dCDP) and 120 μg/L (CDP, dCDP, CMP) ERY treatments (Appendix A **Tables S4-S5**). In addition, cytidine deaminase (ecoded by *cdd*) cytidine deaminase catalyzes the deamination of cytidine and 2′-deoxycytidine to produce uridine and deoxyuridine, respectively (Bharat et al., 2019). Uridine kinase (encoded by *udk*) catalyzes the phosphorylation of uridine and cytidine to UMP and CMP, respectively (Zrenner et al., 2006). The upregulation of *cdd* and *udk* was associated with reduced contents of uridine and deoxyuridine in both the 80 and 120 μg/L ERY treatments (Appendix A **Tables S4-S5**). The dysregulation of pyridine metabolism may also contribute to the growth inhibition in algae treated with 80 and 120 μg/L ERY.

4. Conclusions

Exposure to ERY caused a dose-dependent metabolomic response in *R. subcapitata*. Growth promotion induced by 4 μg/L ERY treatment was associated with metabolomic pathways including ABC transporters, fatty acid biosynthesis and purine metabolism. By contrast, growth inhibition induced by 80 and 120 μg/L ERY treatments was likely due to the dysregulation of metabolomic pathways including ABC transporters, 2-oxocarboxylic acid metabolism, glyoxylate and dicarboxylate metabolism, biosynthesis of amino acids, Aminoacyl-tRNA biosynthesis, fatty acid biosynthesis, purine metabolism and pyridine metabolism. Notably, orthogonal experiments (e.g., a two-factor or full factorial design) are warranted to assess the contribution of environmental factors (e.g., light intensity, temperature, pH, salinity nutrients, and contaminants) to the ERY-induced hormesis in algae. In addition, whether and how similar dose-dependent responses can be induced in other algae by ERY (or other antibiotics) warrant for further investigation. This study supported that multi-omics analyses can serve as good supplementary tools to the commonly used apical endpoints for evaluating the toxicity of antibiotics on algae and providing constructive information for environmental risk assessment, as the no observed effect concentration (NOEC) can be affected by the presence of hormesis.

Acknowledgments

This work was supported by theNational Natural Science Foundation of China (No. 42101077), The Key Research and Development Program of ShaanXi Province (No. 2020SF-387), and ShaanXi Thousand Talent Program for Young Outstanding Scientists (No. 334041900007).

Appendix A Supplementary data

Supplementary material associated with this article can be found, in the online version, at doi:10.1016/j.jes.2021.12.001.

REFERENCES

Agathokleous, E., Kitao, M., Calabrese, E.J., 2020. Hormesis: Highly generalizable and beyond laboratory. Trends Plant Sci. 25 (11), 1076–1086.

Aguirre-Martínez, G.V., DelValls, T.A., Martín-Díaz, M.L., 2016. General stress, detoxification pathways, neurotoxicity and genotoxicity evaluated in *Ruditapes philippinarum* exposed to human pharmaceuticals. Ecotoxicol. Environ. Saf. 124, 18–31.

Agunbiade, F.O., Moodley, B., 2014. Pharmaceuticals as emerging organic contaminants in Umgeni River water system, KwaZulu-Natal, South Africa. Environ. Monit. Assess. 186 (11), 7273–7291.

Akram, M., Asif, H.M., Uzair, M., Akhtar, N., Madni, A., Shah, S.A., et al., 2011. Amino acids: A review article. J. Med. Plant Res. 5 (17), 3997–4000.

Aliferis, K.A., Jabaji, S., 2011. Metabolomics–a robust bioanalytical approach for the discovery of the modes-of-action of pesticides: a review. Pestic. Biochem. Physiol. 100 (2), 105–117.

Ambasht, P.K., Kayastha, A.M., 2002. Plant pyruvate kinase. Biol. Plant. 45 (1), 1–10.

Andolfo, G., Ruocco, M., Di Donato, A., Frusciante, L., Lorito, M., Scala, F., et al., 2015. Genetic variability and evolutionary diversification of membrane ABC transporters in plants. BMC Plant Biol. 15 (1), 1–15.

Arenz, S., Ramu, H., Gupta, P., Berninghausen, O., Beckmann, R., Vázquez-Laslop, N., et al., 2014. Molecular basis for erythromycin-dependent ribosome stalling during translation of the ErmBL leader peptide. Nat. Commun. 5 (1), 1–8.

Bai, Y., Meng, W., Xu, J., Zhang, Y., Guo, C., 2014. Occurrence, distribution and bioaccumulation of antibiotics in the Liao River Basin in China. Environ. Sci.-Proc. Imp. 16 (3), 586–593.

Bharat, S.S., Li, S., Li, J., Yan, L., Xia, L., 2019. Base editing in plants: current status and challenges. Crop J. 8 (3), 384–395.

Binder, S., Knill, T., Schuster, J., 2007. Branched-chain amino acid metabolism in higher plants. Physiol. Plant. 129 (1), 68–78.

Burch, L.R., Stuchbury, T., 1987. Activity and distribution of enzymes that interconvert purine bases, ribosides and ribotides in the tomato plant and possible implications for cytokinin metabolism. Physiol. Plant. 69 (2), 283–288.

Cagliari, A., Margis, R., dos Santos Maraschin, F., Turchetto-Zolet, A.C., Loss, G., Margis-Pinheiro, M., 2011. Biosynthesis of triacylglycerols (TAGs) in plants and algae. Int. J. Plant Biol. 2 (1), e10.

Calabrese, E.J., 2010. Hormesis is central to toxicology, pharmacology and risk assessment. Hum. Exp. Toxicol. 29 (4), 249–261.

Chitrakar, I., Kim-Holzapfel, D.M., Zhou, W., French, J.B., 2017. Higher order structures in purine and pyrimidine metabolism. J. Struct. Biol. 197 (3), 354–364.

Dahuja, A., Kumar, R.R., Sakhare, A., Watts, A., Singh, B., Goswami, S., et al., 2021. Role of ATP-binding cassette transporters in maintaining plant homeostasis under abiotic and biotic stresses. Physiol. Plant. 171 (4), 785–801.

Dashty, M., 2013. A quick look at biochemistry: carbohydrate metabolism. Clin. Biochem. 46 (15), 1339–1352.

de la Torre, F., Cañas, R.A., Pascual, M.B., Avila, C., Cánovas, F.M., 2014. Plastidic aspartate aminotransferases and the biosynthesis of essential amino acids in plants. J. Exp. Bot. 65 (19), 5527–5534.

Deng, C.N., Zhang, D.Y., Pan, X.L., 2014. Toxic effects of erythromycin on photosystem I and II in *Microcystis aeruginosa*. Photosynthetica 52 (4), 574–580.

Etienne, A., Génard, M., Lobit, P., Mbeguié-A-Mbéguié, D., Bugaud, C., 2013. What controls fleshy fruit acidity? A review of malate and citrate accumulation in fruit cells. J. Exp. Bot. 64 (6), 1451–1469.

Gaynor, M., Mankin, A.S., 2003. Macrolide antibiotics: binding site, mechanism of action, resistance. Curr. Top. Med. Chem. 3 (9), 949–960.

Guo, J., Boxall, A., Selby, K., 2015. Do pharmaceuticals pose a threat to primary producers? Crit. Rev. Environ. Sci. Technol. 45 (23), 2565–2610.

Guo, J., Ma, Z., Peng, J., Mo, J., Li, Q., Guo, J., et al., 2021. Transcriptomic analysis of *Raphidocelis subcapitata* exposed to erythromycin: The role of DNA replication in hormesis and growth inhibition. J. Hazard. Mater. 402, 123512.

Guo, J., Selby, K., Boxall, A.B., 2016. Assessment of the risks of mixtures of major use veterinary antibiotics in European surface waters. Environ. Sci. Technol. 50 (15), 8282–8289.

Guschina, I.A., Harwood, J.L., 2006. Lipids and lipid metabolism in eukaryotic algae. Prog. Lipid Res. 45 (2), 160–186.

Hall, M.B., Mertens, D.R., 2017. A 100-year review: carbohydrates—characterization, digestion, and utilization. Int. J. Dairy Sci. 100 (12), 10078–10093.

Ibba, M., Söll, D., 2000. Aminoacyl-tRNA synthesis. Annu. Rev. Biochem. 69 (1), 617–650.

Igamberdiev, A.U., Eprintsev, A.T., 2016. Organic acids: the pools of fixed carbon involved in redox regulation and energy balance in higher plants. Front. Plant Sci. 7, 1042.
Jamers, A., Blust, R., De Coen, W., 2009. Omics in algae: paving the way for a systems biological understanding of algal stress phenomena? Aquat. Toxicol. 92 (3), 114–121.
Jelić, D., Antolović, R., 2016. From erythromycin to azithromycin and new potential ribosome-binding antimicrobials. Antibiotics 5 (3), 29.
Kafer, C., Zhou, L., Santoso, D., Guirgis, A., Weers, B., Park, S., et al., 2004. Regulation of pyrimidine metabolism in plants. Front. Biosci. 9, 1611–1625.
Kamerlin, S.C., Sharma, P.K., Prasad, R.B., Warshel, A., 2013. Why nature really chose phosphate. Q. Rev. Biophys. 46 (1), 1–132.
Kanehisa, M., Sato, Y., Kawashima, M., Furumichi, M., Tanabe, M., 2016. KEGG as a reference resource for gene and protein annotation. Nucleic Acids Res. 44, D457–D462.
Kang, J., Park, J., Choi, H., Burla, B., Kretzschmar, T., Lee, Y., et al., 2011. Plant ABC transporters. Arabidopsis book/Am. Soc. Plant Biol. 9.
Kumar, M., Jaiswal, S., Sodhi, K.K., Shree, P., Singh, D.K., Agrawal, P.K., et al., 2019. Antibiotics bioremediation: Perspectives on its ecotoxicity and resistance. Environ. Int. 124, 448–461.
Lea, P.J., Miflin, B.J., 2003. Glutamate synthase and the synthesis of glutamate in plants. Plant Physiol. Biochem. 41 (6-7), 555–564.
Li, Q., Cheng, B., Liu, S., Zhang, Y., Zhou, L., Guo, J., 2020. Assessment of the risks of the major use antibiotics in China's surface waters using a probabilistic approach. Integr. Environ. Assess. Manag. 16 (1), 43–52.
Li, X., Peng, T., Mu, L., Hu, X., 2019. Phytotoxicity induced by engineered nanomaterials as explored by metabolomics: perspectives and challenges. Ecotoxicol. Environ. Saf. 184, 109602.
Liang, R., Shao, X., Shi, Y., Jiang, L., Han, G., 2020. Antioxidant defenses and metabolic responses of blue mussels (*Mytilus edulis*) exposed to various concentrations of erythromycin. Sci. Total Environ. 698, 134221.
Li-Beisson, Y., Thelen, J.J., Fedosejevs, E., Harwood, J.L., 2019. The lipid biochemistry of eukaryotic algae. Prog. Lipid Res. 74, 31–68.
Lin, A.Y.C., Tsai, Y.T., 2009. Occurrence of pharmaceuticals in Taiwan's surface waters: Impact of waste streams from hospitals and pharmaceutical production facilities. Sci. Total Environ. 407 (12), 3793–3802.
Liu, B.Y., Nie, X.P., Liu, W.Q., Snoeijs, P., Guan, C., Tsui, M.T., 2011a. Toxic effects of erythromycin, ciprofloxacin and sulfamethoxazole on photosynthetic apparatus in *Selenastrum capricornutum*. Ecotoxicol. Environ. Saf. 74 (4), 1027–1035.
Liu, B., Liu, W., Nie, X., Guan, C., Yang, Y., Wang, Z., et al., 2011b. Growth response and toxic effects of three antibiotics on *Selenastrum capricornutum* evaluated by photosynthetic rate and chlorophyll biosynthesis. J. Environ. Sci. 23 (9), 1558–1563.
Liu, J., Lu, G., Ding, J., Zhang, Z., Wang, Y., 2014. Tissue distribution, bioconcentration, metabolism, and effects of erythromycin in crucian carp (*Carassius auratus*). Sci. Total Environ. 490, 914–920.
Loos, R., Marinov, D., Sanseverino, I., Napierska, D., Lettieri, T., 2018. Review of the 1st watch list under the water framework directive and recommendations for the 2nd watch list. Luxembourg 1–268.
Ma, Z., Yang, F., Ren, J., Fan, R., Duan, Q., Guo, J., et al., 2021. Growth inhibition and oxidative stress in two green algal species exposed to erythromycin. J. Am. Water Resour. Assoc. 57 (4), 628–637.
Machado, M.D., Soares, E.V., 2019. Impact of erythromycin on a non-target organism: cellular effects on the freshwater microalga *Pseudokirchneriella subcapitata*. Aquat. Toxicol. 208, 179–186.
Martinez, J.L., 2009. Environmental pollution by antibiotics and by antibiotic resistance determinants. Environ. Pollut. 157 (11), 2893–2902.
Matich, E.K., Soria, N.G.C., Aga, D.S., Atilla-Gokcumen, G.E., 2019. Applications of metabolomics in assessing ecological effects of emerging contaminants and pollutants on plants. J. Hazard. Mater. 373, 527–535.
Miao, X.S., Bishay, F., Chen, M., Metcalfe, C.D., 2004. Occurrence of antimicrobials in the final effluents of wastewater treatment plants in Canada. Environ. Sci. Technol. 38 (13), 3533–3541.
Moffatt, B.A., McWhinnie, E.A., Agarwal, S.K., Schaff, D.A., 1994. The adenine phosphoribosyltransferase-encoding gene of *Arabidopsis thaliana*. Gene 143 (2), 211–216.
Nägele, T., 2014. Linking metabolomics data to underlying metabolic regulation. Front. Mol. Biosci. 1, 22.
Nie, X.P., Liu, B.Y., Yu, H.J., Liu, W.Q., Yang, Y.F., 2013. Toxic effects of erythromycin, ciprofloxacin and sulfamethoxazole exposure to the antioxidant system in *Pseudokirchneriella subcapitata*. Environ. Pollut. 172, 23–32.
OECD, 2011. OECD (Organization for Economic Co-operation and Development) 201 guidelines for the testing of chemicals, Freshwater Alga and Cyanobacteria. Growth Inhibition Test. https://www.oecd-ilibrary.org/environment/test-no-201-alga-growth-inhibition-test_9789264069923-en. May 15, 2020 Accessed.
Patel, M.S., Korotchkina, L.G., 2003. The biochemistry of the pyruvate dehydrogenase complex. Biochem. Mol. Biol. Educ. 31 (1), 5–15.
Peng, J., Guo, J., Lei, Y., Mo, J., Sun, H., Song, J., 2021. Integrative analyses of transcriptomics and metabolomics in *Raphidocelis subcapitata* treated with clarithromycin. Chemosphere 266, 128933.
Raghothama, K.G., 2000. Phosphate transport and signaling. Curr. Opin. Plant Biol. 3 (3), 182–187.
Raman, S.B., Rathinasabapathi, B., 2004. Pantothenate synthesis in plants. Plant Sci. 167 (5), 961–968.
Rodrigues, S., Antunes, S.C., Correia, A.T., Nunes, B., 2016. Acute and chronic effects of erythromycin exposure on oxidative stress and genotoxicity parameters of *Oncorhynchus mykiss*. Sci. Total Environ. 545, 591–600.
Rodrigues, S., Antunes, S.C., Correia, A.T., Nunes, B., 2019. Toxicity of erythromycin to *Oncorhynchus mykiss* at different biochemical levels: detoxification metabolism, energetic balance, and neurological impairment. Environ. Sci. Pollut. Res. 26 (1), 227–239.
Schafhauser, B.H., Kristofco, L.A., de Oliveira, C.M.R., Brooks, B.W., 2018. Global review and analysis of erythromycin in the environment: occurrence, bioaccumulation and antibiotic resistance hazards. Environ. Pollut. 238, 440–451.
Sendra, M., Damián-Serrano, A., Araújo, C.V., Moreno-Garrido, I., Blasco, J., 2018. Erythromycin sensitivity across different taxa of marine phytoplankton. A novel approach to sensitivity of microalgae and the evolutionary history of the 23S gene. Aquat. Toxicol. 204, 190–196.
Shafia, S., Chandluri, P., Ganpisetti, R., Lakshmi, B.V.S., Swami, P.A., 2016. Erythrmycin use as broad spectrum antibiotic. World J. Pharm. Med. Res. 2 (6), 23–26.
Slaveykova, V.I., Majumdar, S., Regier, N., Li, W., Keller, A.A., 2021. Metabolomic responses of green alga *Chlamydomonas reinhardtii* exposed to sublethal concentrations of inorganic and methylmercury. Environ. Sci. Technol. 55 (6), 3876–3887.

Stasolla, C., Katahira, R., Thorpe, T.A., Ashihara, H., 2003. Purine and pyrimidine nucleotide metabolism in higher plants. J. Plant Physiol. 160 (11), 1271–1295.

Stottmeister, U., Aurich, A., Wilde, H., Andersch, J., Schmidt, S., Sicker, D., 2005. White biotechnology for green chemistry: fermentative 2-oxocarboxylic acids as novel building blocks for subsequent chemical syntheses. J. Ind. Microbiol. Biotechnol. 32 (11–12), 651–664.

Suzuki, S., Yamaguchi, H., Nakajima, N., Kawachi, M., 2018. *Raphidocelis subcapitata* (= *Pseudokirchneriella subcapitata*) provides an insight into genome evolution and environmental adaptations in the Sphaeropleales. Sci. Rep. 8 (1), 1–13.

Thomas, C., Aller, S.G., Beis, K., Carpenter, E.P., Martinoia, E., 2020. Structural and functional diversity calls for a new classification of ABC transporters. FEBS Lett. 594 (23), 3767–3775.

Valcárcel, Y., Alonso, S.G., Rodríguez-Gil, J.L., Gil, A., Catalá, M., 2011. Detection of pharmaceutically active compounds in the rivers and tap water of the Madrid Region (Spain) and potential ecotoxicological risk. Chemosphere 84 (10), 1336–1348.

Voelker, T., 1996. Plant acyl-ACP thioesterases: chain-length determining enzymes in plant fatty acid biosynthesis. Genet. Eng. 111–133.

Wan, J., Guo, P., Peng, X., Wen, K., 2015. Effect of erythromycin exposure on the growth, antioxidant system and photosynthesis of *Microcystis flos-aquae*. J. Hazard. Mater. 283, 778–786.

Wan, X., Wu, S., Li, Z., An, X., Tian, Y., 2020. Lipid metabolism: Critical roles in male fertility and other aspects of reproductive development in plants. Mol. Plant. 3 (7), 955–983.

Ward, P.S., Thompson, C.B., 2012. Signaling in control of cell growth and metabolism. Cold Spring Harb. Perspect. Biol. 4 (7), a006783.

Wiegand, G., Remington, S.J., 1986. Citrate synthase: structure, control, and mechanism. Annu. Rev. Biophys. 15 (1), 97–117.

Xiao, W., Wang, R.S., Handy, D.E., Loscalzo, J., 2018. NAD(H) and NADP(H) redox couples and cellular energy metabolism. Antioxid. Redox Signal. 28 (3), 251–272.

Yalcinkaya, T., Uzilday, B., Ozgur, R., Turkan, I., Mano, J.I., 2019. Lipid peroxidation-derived reactive carbonyl species (RCS): Their interaction with ROS and cellular redox during environmental stresses. Environ. Exp. Bot. 165, 139–149.

Yoshinobu, F., Yomoaki, F., Yuko, Y., Yasue, S., Yoshinobo, K., Yoshikazu, T., 1983. Physical characterization of erythromycin dihydrate, anhydrate and amorphous solid and their dissolution properties. Chem. Pharm. Bull. 31, 4029–4039.

Zainab, S.M., Junaid, M., Xu, N., Malik, R.N., 2020. Antibiotics and antibiotic resistant genes (ARGs) in groundwater: A global review on dissemination, sources, interactions, environmental and human health risks. Water Res., 116455.